CHAPTER 4

PIC SIMULATION OF A GYRO-TWT AMPLIFIERS

4.1. Introduction

The electron beam and RF wave interaction mechanism is relatively a complex phenomena in non-uniform interaction circuit as there are number of parameters which affect the output performance of the amplifier. For the validation of the analytical results, the PIC simulation codes are used for the study of the beam-wave interaction phenomenon in the fast-wave electron-beam devices including, gyrotron, gyro-TWT, gyro-klystron, etc. [Wu *et al.* (1996), Barroso *et al.* (1999), Song *et al.* (2004), Kory and Dayton (2009), Reddy *et al.* (2008), Reddy *et al.* (2010), Xu *et al.* (2010), Xu *et al.* (2011), Kumar *et al.* (2011), Yan *et al.* (2012), Du *et al.* (2013), Thottappan *et al.* (2013), Yan *et al.* (2014), Li *et al.* (2014), Wang *et al.* (2014)]. By considering the nearby competing modes, the PIC simulation assists us to have an in-depth understanding of the EM behaviour of the device.

Initially, through eigenmode solver interaction region is cold simulated for its EM behaviour by confirming the establishment of the desired operating mode as well as desired frequency. The real performance of the amplifier could be realized under practical condition, i.e., under beam present condition using a commercially available advanced 3D PIC codes, like, MAGIC, MAFIA, CST Studio Suite, CHIPIC etc. These codes give overall understanding of the complex beam-wave interaction process in any vacuum electron devices. Kory has presented the 3D PIC simulation module of MAFIA for investigating the interaction mechanism in a helix TWT amplifier [Kory (2001)]. In 2009, Kory used PIC module of CST Particle Studio for the designing of 650GHz helical BWO [Kory *et al.* (2008)]. At present, some of the researchers using the PIC codes for beam-wave interaction simulation of gyrotron and gyro-TWT, such as, simulation of a high power 390GHz large-orbit harmonic gyrotron are performed using 3D MAGIC PIC code [Li (2009)].

In order to validate and examine the accuracy of "CST PIC simulation code" and its efficient use in gyro-TWT, the RF behaviour of 35GHz, Ka-band, fundamental harmonic TE_{01} mode gyro-TWT having a smooth wall cylindrical waveguide and a fundamental harmonic, 92GHz, TE_{01} heavy loaded waveguide interaction structure independently is presented. A commercial code "CST particle studio" is reconfigured for the gyro-TWT structure condition and electrical condition to explore the beam-wave interaction mechanism of the gyro-TWT [CST user's manual (2014)]. Recently "CST Particle studio" has been used to simulate a Ka-band gyro-TWT [Reddy *et al.* (2010)], and 92.5GHz fundamental harmonic TE_{01} mode [Tang *et al.* (2014)].

The 3D CST particle studio code has a powerful graphical user interface (GUI) based simulation software. Through this simulation code, the signal amplitudes of all modes in the cylindrical waveguide of the gyro-TWT could be observed in interaction region simultaneously, which provide a more practical situation. The field values are recorded in the time domain and after post processing; its Fourier transform provides the device frequency of operation at the desired mode. The electron particle beamlets at different time intervals within one cycle are shown to understand the bunching mechanism. The energy distribution of all the particles along the interaction length is demonstrated to understand the energy transfer phenomena between the wave and beam. The effect of velocity spread, pitch factor and input frequencies on the device performance is also described. Beam-wave interaction yields the temporal RF power growth at the output end of the interaction structure. The stability of the device is also discussed. It is observed that the presence of competing modes affects the gyro-TWT performance. The overall performances of the

conventional and heavily loaded gyro-TWT have been observed in terms of output power and efficiency is described.

In this chapter, section 4.2 describes the basic description of "Numerical Techniques" and its features. Section 4.3 deals with the PIC simulation and modelling of a fundamental Ka-band conventional gyro-TWT. In section 4.4, the results are discussed with parametric analysis and validation. In section 4.5, discussed the modelling of heavily loaded W-band fundamental harmonic gyro-TWT is investigated. Section 4.6 discusses the results of PIC results of a W-band, fundamental harmonic gyro-TWT amplifier. The conclusions are drawn in section 4.7.

4.2. PIC Simulation Description

The interaction between the electromagnetic fields and charged particles in a vacuum electronic device is well described by the equations of classical physics. That is, the fields are determined by Maxwell's equations with source current and charge densities; while the electrons and other charged particles are governed by Newton's laws or their relativistic generalizations [Antonsen *et al.* (1999)]. Obviously, these equations are coupled together in that the electromagnetic fields are driven by the currents and charges of the moving electrons, while the electrons move in response to the electromagnetic fields. Numerical techniques have made upgrading in the field of electromagnetic applications. The PIC method has origins in electron trajectory simulation, with the first work in plasmas in the 1950's [Dawson (1959), Buneman (1962)]. Early work did not use a grid for the fields, resulting in lengthy calculations. The PIC method, adding a numerical grid for the fields, was formalized and codified, including the theory of simulation, in the 1960's–1980 [Birdsall and Bruce (1985), Hockney and Eastwood (1981)]. In the present time, the design

and analysis of electromagnetic problems needs consistent, precise and flexible simulation tools. Computer techniques for investigating the electromagnetic problems fall into one of three categories, analytical methods, numerical methods, and expert systems. Analytical methods are appropriate for simple and uniform structure. Numerical methods can be applied for complex and heterogeneous geometries. Expert systems do not actually calculate the field directly, but instead estimate values for the parameters of interest. Numerical techniques require more calculation than other two methods but they are powerful simulation tools. There are numerous of numerical techniques (HFSS, MAGIC, MAFIA, CHIPIC, CST, etc.) are available for solving electromagnetic distribution problems and each method is well suited for the analysis of a particular type of problem and a variety of numerical techniques are being used for the beam-wave interaction calculation. The most widely used to techniques are the finite-difference-time-domain (FDTD) method, the finite integration technique (FIT), the finite-element method (FEM), and the method of moments (MoM). The FIT method has been used for applications over an extremely wide range of frequencies, from DC to THz.

The CST is a general purpose electromagnetic simulator based on the finite integration technique (FIT) and which was first proposed by Weiland in 1977. This numerical method provides a universal spatial discretization scheme, applicable to various electromagnetic problems, ranging from static field calculations to high frequency applications in time or frequency domain. Unlike most numerical methods, FIT discretizes the integral form of Maxwell's equations, rather than the differential one. In order to solve these equations numerically a finite calculation domain is defined, enclosing the considered application problem. By creating a suitable mesh system, this domain is split up into

several small cuboids. However, internally a second or dual mesh is set up orthogonally to the first one. The spatial discretization of Maxwell's equations is finally performed on these two orthogonal grid systems. The FIT belongs to the class of local approach in the sense, that the discrete equations are derived cell-by-cell by transforming the continuous Maxwell's equations on to the computational grid. Other representatives of local approaches are Finite Differences (FD), Finite Volumes (FV), Finite Elements (FE), and the Cell Method (CM). All these approaches are based on a volume discretization, defined by the three-dimensional mesh.

The FIT based CST particle studio is a 3D electromagnetic simulation tool which has been extensively used for studying the beam-wave interaction mechanism in most of the electron beam devices due to the simple and efficient algorithm. This software has a special feature called perfect boundary approximation (PBA), which allows mesh cells to be partially filled. It has also been well suited to these applications because it can efficiently model the mixed geometries. The 3D CST PIC studio uses the hexahedral/tetrahedral meshing technique for discretizing the computational domain and which is also user friendly interface for analysing results with its post-processing module. Another PIC code is MAGIC and which is a user configurable one based on FDTD method. This tool calculates desired mode at a time, its computational time is less but the CST particle studio calculates the multiple modes (desired and competing) simultaneously and which is a GUI based 3-D simulation code. Some of the results obtained by transient analysis can be verified by eigenmode solver.

Transient solver: Some of the typical applications where transient solver can be used are: Scattering parameter matrices (S-parameter), Electromagnetic field distributions at various

frequencies, Signal analysis such as rise times, cross talks etc. including a spice network extraction, Structure design by using the optimizer or the parameter sweep, Time domain reflectometry, Antenna radiation patterns and relevant antenna parameters, and Radar cross section calculations using far field/RCS monitors [CST user's manual (2014)].

Time domain solver: calculates the development of fields through time at discrete locations and at discrete time samples. It calculates the transmission of energy between various ports and/or open space of the investigated structure.

The fields are calculated step by step through time by the "Leap Frog" updating scheme. It is proven that this method remains stable if the step width for the integration does not overcome a known limit. This value of the maximum usable time step is directly related to the minimum mesh step width used in the discretization of the structure. Therefore, the denser the chosen grid, the smaller the usable time step width.

Before starting the solver, one should make all necessary settings. The structure is constructed by only using primitive shapes such as cylinders. Different materials are defined and applied which need to exhibit thermal conductivities as well as electric losses.

1. Units: The units of the calculation are to be set i.e., units for frequency, dimensions, time, temperature etc. When a parameter is changed, all expressions including this unit will be multiplied with the unit factor.

2. Background materials: These are the material properties of the background material. The following material types are available:

PEC Sets the background material to a Perfect Electric Conductor.

Normal Sets the background material to a normal material which is loss free and determined by its Epsilon and Mue.

Epsilon/Mue These values are permittivity *Epsilon* and permeability *Mue* if the normal material type is selected.

3. Frequency: No meshing is done, without a valid frequency range of operation and therefore no calculation is possible without specifying the frequency range. The upper frequency of calculation defines the minimum mesh step.

4. Boundary Condition: Due to the fact that a computer is only capable of calculating problems that have finite expansion, you need to specify the boundary conditions. Six boundary types are available like electric, magnetic, periodic, open (PML), open (add space), unit cell and conducting wall.

5. Excitation Source: The S-matrix describes the transmission of electromagnetic field energy between different ports of a structure. Two different kinds of ports exist: Waveguide ports and discrete ports. For the excitation of the transient simulation two waveguide ports are used at the ends of the structure.

6. Field monitors: This gives an opportunity to define field monitors that one might need to obtain additional information on the electromagnetic field distribution inside a structure. Different types of field monitors like, E-field, H-field (surface current) and power flow are available.

7. PIC position monitor: Three types of phase monitor (PIC position monitor, PIC phase space monitor and PIC 2D monitor) are available in 3D CST. It gives the information about the phase at all interaction time.

8. Mesh generation: After the model is setup geometrically and assigned the appropriate power sources and boundary conditions, the calculation domain has to be subdivided into small cells on which Maxwell's grid Equations must be solved. Microwave Studio uses

either the FI formulation on orthogonal Cartesian grids or on tetrahedral grids. The mesh influences the accuracy and speed of the simulation. There are three ways of mesh generation, manual, automatic and adaptive mesh refinement.

9. Post processing: Performing a transient calculation using waveguide ports the resulting time signals are converted automatically into the desired scattering parameters. All these results are listed in the navigation tree in the folder '1D Results' and demonstrate the wave propagation of the filter. Furthermore the results of the electric field monitor are stored in the folder '2D/3D Results', where also the calculated port modes of the given waveguide ports can examined.

10. Eigenmode solver: First the model is created with several periods and truncated in the longitudinal boundaries with electric (E) or magnetic (M) walls. A perfect conductor is simulated by using electric wall, which forces the electric field to be perpendicular to this boundary. Similarly at a magnetic boundary the magnetic field is forced to become perpendicular to this boundary. To reduce the computation time symmetries can be defined in *xy*, *yz* and *zx* planes. Some of the eigenmode parameters that can be set from the solve menu are number of modes desired, frequency, number of iterations and accuracy. Generally these parameters can be left as default settings, but if higher accuracy is needed some have these parameters had to be set**.**

The salient features of "CST Microwave studio" are its diagnosis of results and post-processing module. It provides users to employ six different field solvers, electrostatic, magneto-static, eigen mode solver, particle tracking solver, particle-in-cell solver (PIC) and wake-field solver. In cases of strongly resonant loss-free structures, where the fields (the modes) are to be calculated, the Eigenmode solver is very efficient. The Eigenmode solver

cannot be used with open boundaries or discrete ports [CST user's manual (2014)]. Magneto-static solver can be used for static magnetic problems while Electrostatic solver can be used for static electric problems. Both of these solvers utilizes feature of open boundary conditions. These help to reduce the number of mesh nodes, when problems in free space are simulated. The gun and particle tracking solver can be used to compute trajectories of charged particles within electrostatic, magneto-static or Eigen mode fields. A self-consistent electrostatic field is calculated using gun-iteration implemented which considers the reaction of the particle movement to the electrostatic potential distribution. Particle sources can be defined at arbitrary surface of solids that emits particles according to the predefined emission models. The major task for the tracking solver is to calculate the particle trajectories, the self-consistent electrostatic field, the space charge distribution and the particles current. These results appear automatically in the navigation tree after the solver run. The particle tracking solver also offers the tracking of different types of particle from different sources independently. Thus, multi-beam guns or the parallel simulation of particle beams can be simulated. The computation of wake-potentials of charged particle bunches can be performed using the wake-field solver. For the designing of particle-accelerators, wake-potentials provide important information.

The PIC solver simulates the evolution of charged particles in self-consistent electromagnetic fields. Moreover, in the PIC simulation, the static or analytic field distributions can easily be added. CST Particle Studio also involves four major steps before proceeding for the solution of beam-wave interaction problems. The basic steps in the particle simulation (beam present simulation) of RF interaction circuit using PIC solver are described below[CST user's manual (2014)]. In the CST particle studio, initially, 3D

electromagnetic circuit has to be defined with the required specifications. In the present problem, a conventional cylindrical waveguide as an RF circuit is chosen and its specifications are given in Table 4.1.

For the beam absent analysis, electromagnetic circuit is simulated using eigenmode solver of the CST microwave studio. A desired cross section of an electron beam is injected into the electromagnetic structure, in order to make the interaction between the beam and the RF signal. The dimension of the beam is decided according to the circuit dimension and the desired operating mode. The parameters for developing the electron beam are also defined. A suitable electron optic model is chosen for the problem concern. According to hexahedral mesh surface generated, the emission of particles is defined and controlled.

More number of mesh cells can give higher accuracy with higher emission of particles but it requires more computational time and memory. The current must be approached to its peak value, so that the simulation run is stable. Here, the DC beam emission model is taken which requires assigning any of the constant value parameter to the particles as Lorentz factor (γ), normalized velocity (β), velocity (v) or energy (E_e). These parameters can be calculated as,

$$\gamma = 1 + eV_b / m_0 c^2 \qquad (4.1)$$

$$\beta = \sqrt{1 - \left(1/\gamma^2\right)} \qquad (4.2)$$

The axial electron spread for the particle emission and its velocity can be introduced based on quality of the beam obtained separately by analysis/simulation of a magnetron injection gun (MIG). The external magnetic field is applied to focus the electron beam in a well defined trajectory inside the electromagnetic circuit. The monitors of electric and

magnetic field as well as power developed in the RF structure are defined. Particles are also monitored in 2D or 3D planes to have information about perturbation of the particles in terms of energy or phase and bunching phenomena. Using this monitor commands, particles are monitored at a set interval of time over full or partial time of simulation for their momentum, position, etc. A 2D particle monitor can be set at any of the position in 2D plane mostly at the saturation position or at the entry plane of the collector to acquire the modulation of energy or momentum among particles.

4.3. PIC Simulation of a Ka-Band Fundamental Harmonic Gyro-TWT Amplifier

The beam-wave interaction mechanism in a gyro-TWT employing a smooth wall metal cylindrical waveguide as its RF interaction circuit, initially we have beam absent simulated the circuit in 'CST Microwave studio' so as to ensure the device operation in the desired mode and frequency. After beam absent simulation, the electron beam present simulation has been performed using 'CST Particle studio' which is a particle-in-cell (PIC), taking design parameters as given in Table 4.1.

Table 4.1 Optimized design parameters of Ka-band gyro-TWT amplifier [Seftor *et al.* (1979)]

Particulars	Value
Electron Beam Voltage, V_0	71 kV
Electron Beam Current, I_0	9.5 A
Operating mode, *mn*	TE_{01}
Operating frequency, *f*	35GHz
Velocity pitch, α	1.05
Axial velocity spread	0 %
Circuit radius, R_w	5.5 mm
Guiding center radius, R_g	$0.48R_w$

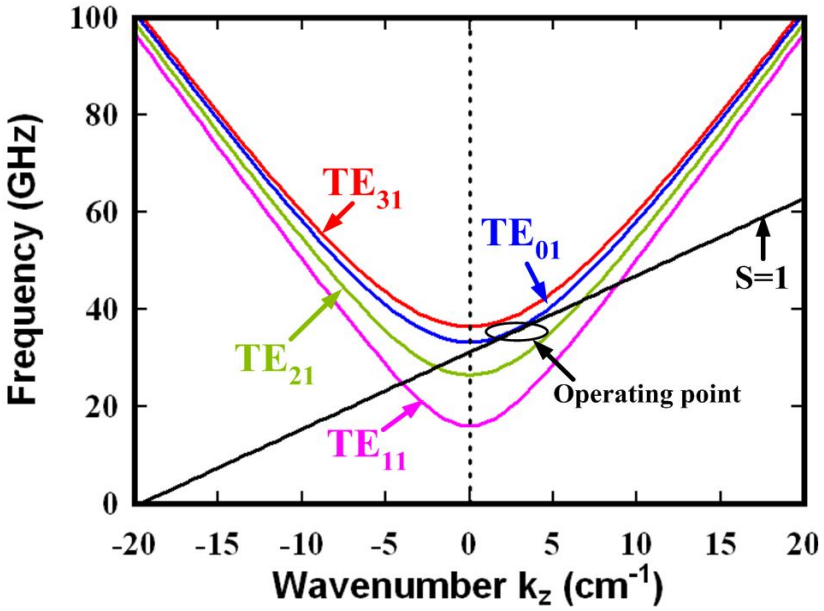

Figure 4.1. Dispersion diagramof Ka-band gyro-TWT with operating and competing modes.

Figure 4.1 shows the dispersion diagram of Ka-band gyro-TWT amplifier. It clearly indicates that the TE_{11} and TE_{21} is nearby competing modes in absolute instability region where $k_z < 0$ and TE_{31} is nearby competing modes in convective instability region where $k_z > 0$. Further, for the beam present simulation, electrons have been considered as uniformly distributed azimuthally in the form of gyrating beamlets and also their evolution along the axial direction of the interaction circuit in presence of electromagnetic signal has been observed in time domain. The boundary condition has been applied as the tangential component of the electric field to be zero. In order to facilitate the simulation process, the space charge effect on the electron beam has been neglected. Electrons start to bunch as they drift along the interaction circuit and as a result, they transfer their energy in synchronism with the Larmor gyration of the electrons. This makes possible amplification of an electromagnetic wave at the cyclotron frequency. Fourier transform of time varying field confirmed the desired frequency of operation in hot beam analysis.

4.3.1. *PIC Interaction Waveguide Modelling*

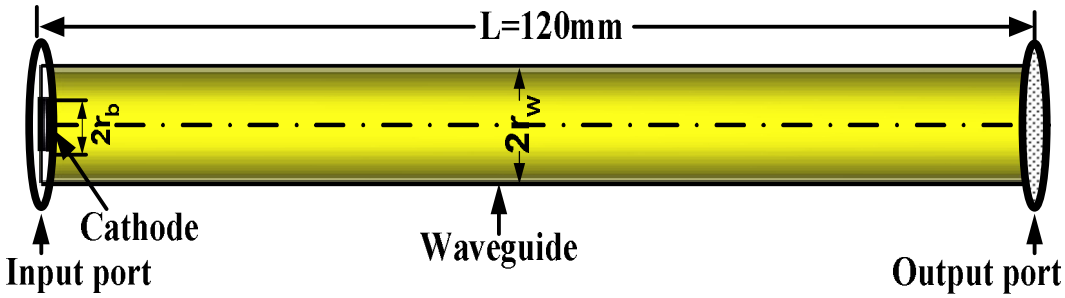

Figure 4.2. Sectional view of the simulation model of Ka-band gyro-TWT.

Figure 4.2 shows the sectional view of Ka-band, simulation model of gyro-TWT amplifier. The interaction structure has been modelled with an annealed oxygen free high conductivity (OFHC) copper material (σ =5.8 x 10^7 S/m). A port has been defined at the output end to observe the signal of any mode (desired as well as competing modes).

4.4. Result and Discussion

4.4.1. Beam Absent (Cold) Simulation

In order to observe the desired mode of operation of the gyro-TWT, the Eigenmode solver of 'CST Microwave studio' has been chosen. Interaction circuit length is 120mm in the propagation direction. As a result of beam absent simulation, the field patterns at different planes of interest as well as EM fields profile along radial and axial positions have been observed. There is no provision in this software to display the specification of the modes, therefore, the existence of various *TE* and *TM* modes are being identified by examining their field distributions. This beam absent simulation confirms the desired mode $TE_{01}$of operation at the desired operating frequency. Figures 4.3 (a) and (b) show the vector and contour plot of electric field intensity inside interaction circuit, respectively, at 35GHz.

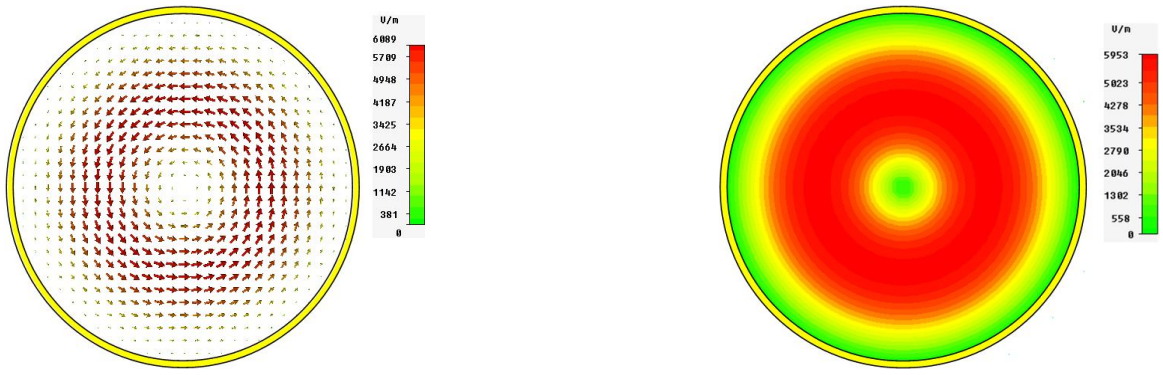

(a) **(b)**

Figure 4.3. (a) Vector plot of Electric field pattern, and **(b)** Contour plots of Electric field of Ka-band gyro-TWT amplifier.

4.4.2. *Beam Present* (*Hot*) *Simulation*

For accuracy, proper meshing should be made for the circuit discretization to obtain good results. In the present work, hexahedral (legacy) meshing has been taken and which is very robust and allows very fast computations with good accuracy.For the study of beam-wave interaction mechanism, the gyrating electron beam has been introduced into the interaction circuit in order to drive the input electromagnetic wave which is to be amplified. Initially, all the particles have been assigned a constant energy value and the current rise time is taken as 1ns. A kinetic spread can be directly introduced into the beam to realize the more reasonable scenario. For the accuracy of results, large number of particles can be considered. Further, field monitors have been setup to observe the waveguide operation in desired mode and frequency, and particles have also been monitored at a desired interval of time over the entire or part of simulation time for their momentum, position, etc.

For the analysis of electron bunch and energy transfer phenomena, phase space for momentum and position of electrons are being recorded as desired. The simulation time has been set as 200ns and four modes have been considered into account to show the mode

competition phenomena in a Ka-band gyro-TWT. The magnetic field is sensitive factors in the beam wave interaction. It determines the coupling strength of the beam wave interaction. An increase in magnetic field may enhance the output power at higher frequency but reduce the output power at the lower frequency due to the excessive saturation of the beam wave interaction. Furthermore, an increase in magnetic field will easily lead to instability of the gyro-TWT. The optimized magnetic field of 1.34T has been kept constant throughout the interaction region. The axial velocity spread has been considered as 0% and also sixteen beamlets have been taken for simulation. In order to improve the accuracy in PIC simulation one should choose the mess size wisely. Lines per wavelength and lower mess limit should be kept so as to get good accuracy in lesser simulation time. The automatic mess generation technique has been used in the present simulation and in which lines per wavelength is taken as 8 and lower mess limit as 7.

4.4.3. *Electron Beam Bunching*

The electrons interact self-consistently with the EM fields present in the interaction circuit. The EM field action is varying with respect to electron relativistic factor (γ), electron phase, and phase slippage and bunching corresponding to current driving the wave. The snapshot of all the particles initial and after the beam-wave interaction inside the waveguide has been shown in Figs. 4.4(a) and 4.4(b). Before interaction, all sixteen beamlets were uniformly distributed with a fixed guiding center radius and their energies were found equal at the starting of interaction process. Figure 4.4(a) also shows that the Larmor radius of all beamlets were same. In Fig. 4.4 (b), bunching of particles can been clearly seen which is due to the change in the Larmour radius during the beam-wave interaction process. Obviously, the presence of EM fields perturb the homogeneity of

helical electron beamlets in the waveguide section and results in the electron bunch formation. This bunch slips into the retarding phase of field, and hence transfers energy to EM field.

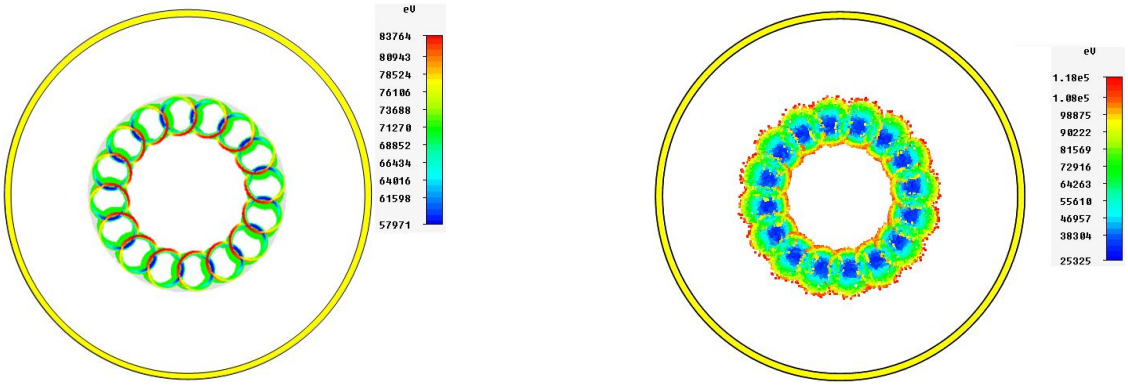

(a) **(b)**

Figure 4.4. Snapshot of electron beamlets **(a)** initial interaction, and **(b)** after interaction of Ka-band gyro-TWT amplifier.

4.4.4. *Output RF Signal and Power*

After the beam-wave interaction TE_{01} and nearby competing mode of operation is observed. The desired mode stable output is obtained at output port and the output power of competing mode is very low. Figure 4.5(a) and 4.5(b) shows the CST 3D particle simulation temporal response of RF output signal amplitude and RF output power of desired and nearby competing mode of gyro-TWT amplifier for RF drive power coupled to the beam having the strength of 10W.

There is a competition between these two modes backward modes (TE_{01} and TE_{21}) and forwarded TE_{03} for the magnetic field of 1.34T and finally TE_{01} mode gets established in the waveguide. On the other hand, TE_{01} mode stabilizes around 80ns in the interaction circuit and then becomes stable. After the template based post processing the output power for the designed parameter has been calculated around 135.5kW.

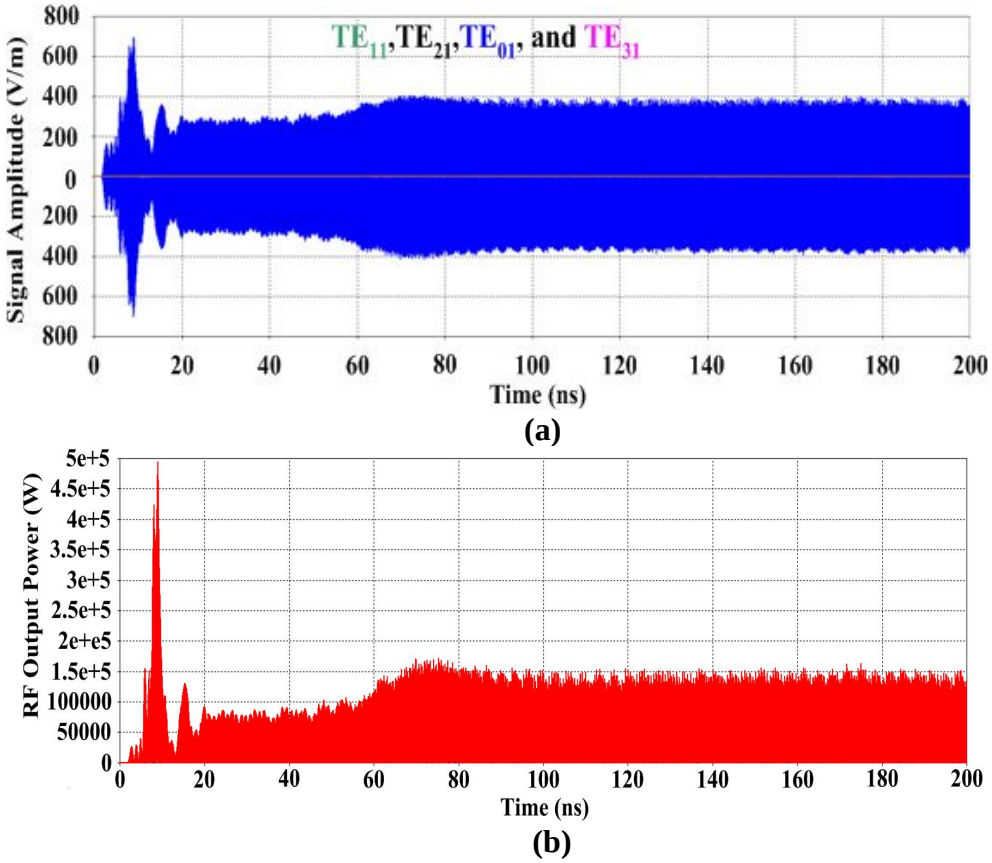

Figure 4.5. (a) Temporal response of output signals amplitude for TE_{01} and it's nearby competing modes, and **(b)** Temporal output power growth at output end for TE_{01} mode.

The total number of electrons coming from the cathode in the whole simulation period is around 80,000 which have been shown in Fig. 4.6 (a). The energy distribution of all electrons has been shown in Fig. 4.6 (b) for 0% velocity spread and which shows that initially all electrons have same energy of 71keV and as time progresses, energy of all particles gets perturbed due to the interaction with RF wave present in the interaction circuit. At the end of interaction circui, majority of particles have lower energy and which represents that particles have lost their energy to RF wave as they come out of interaction circuit and hence the net energy transfer from electrons to the wave taken place. This variation in energy distribution leads to low efficiency and hence the output power. A probe

is placed inside the interaction circuit where the maximum electric field ocuurs and its signal is recorded in time domain. Figures 7(a) and 7(b) depicts the normed momentum at initial (2ns) and after the bunching (200ns).

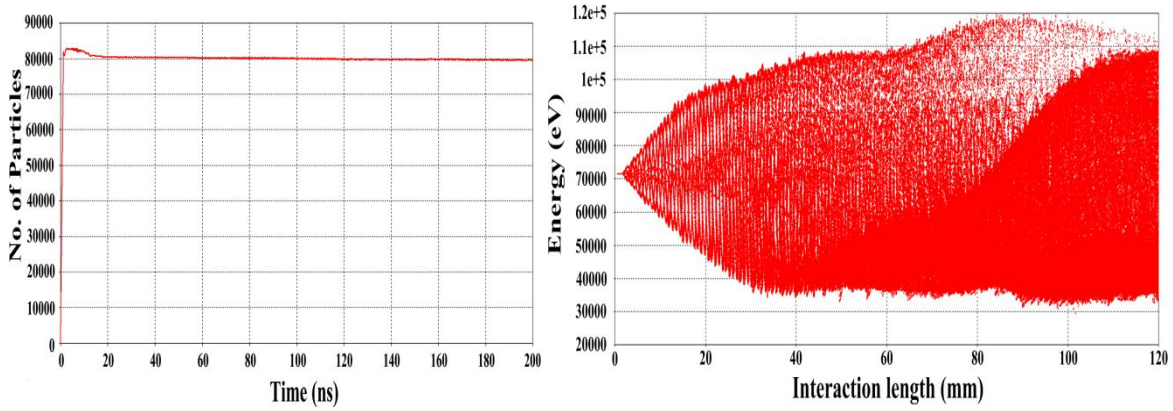

(a) **(b)**

Figure 4.6. (a) Number of particles emitted in 35GHz gyro-TWT amplifier and **(b)** Energy distributions of the electrons in the beam-wave interaction of Ka-band gyro-TWT amplifier.

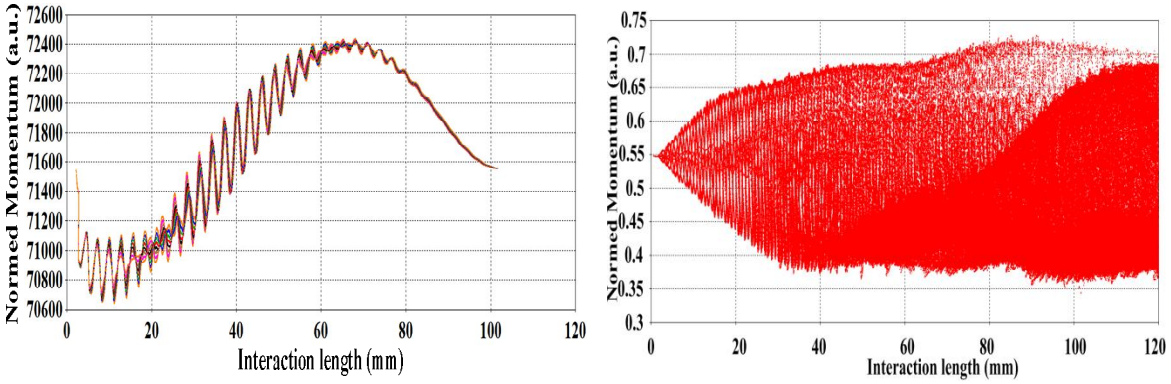

(a) **(b)**

Figure 4.7. (a) Variation of normalized axial momentum before bunching (at 2ns), and (b) Normalized axial momentum after bunching (at 200ns).

Figs. 4.8 shows the frequency spectrum of azimuthal TE_{01} electric field obtained through Fourier transform. Obviously, it is characterized by a single-frequency peaked at 35GHz and this validates the frequency of TE_{01} mode of operation of the gyro- TWT.

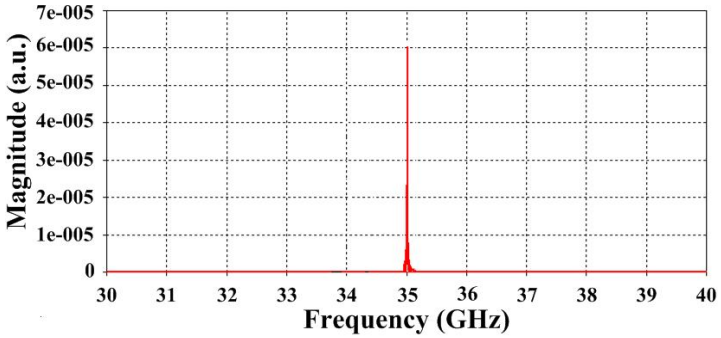

Figure 4.8. Frequency spectrum of probe signal placed inside the interaction circuit.

4.4.5. *Parametric Analysis and Validation*

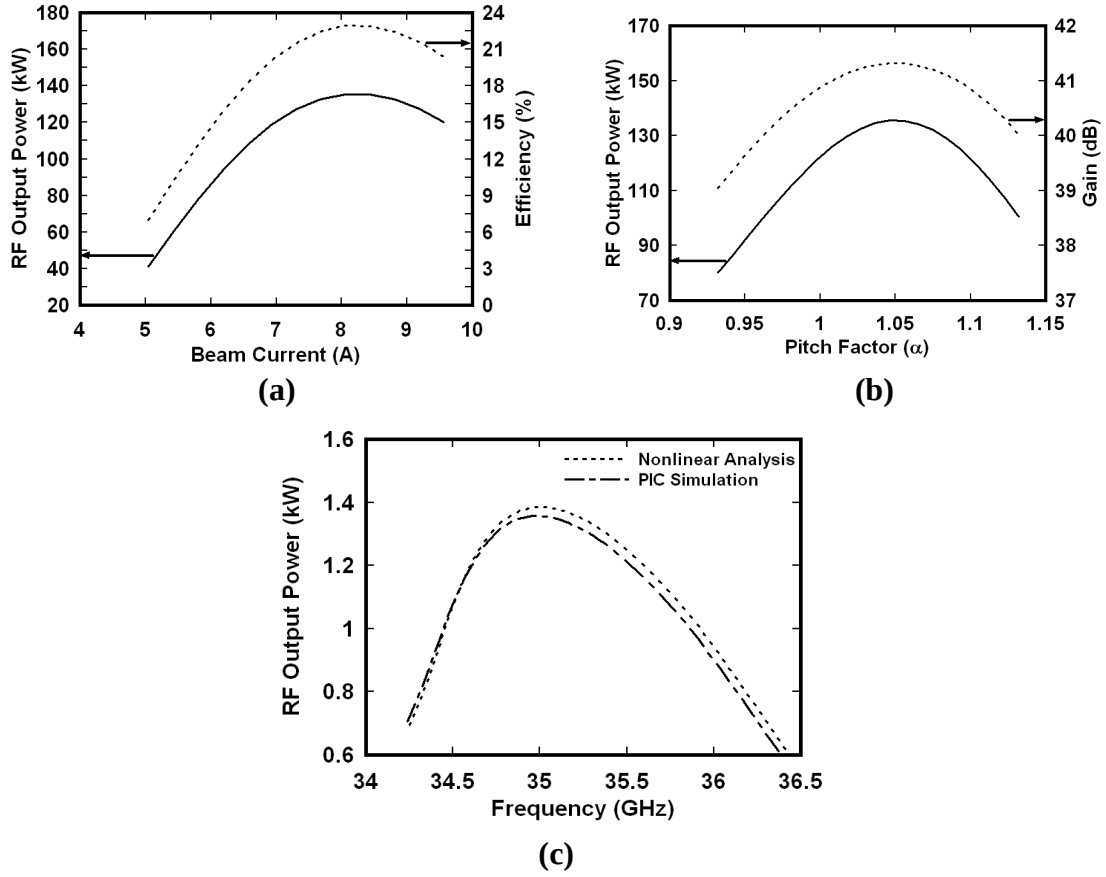

Figure 4.9. (a) Variation of output power and efficiency with beam current, (**b)** Variation of output power and gain with pitch, and **(c)** Variation of output power with frequencies**.**

Figs. 4.9(a) shows the variation of output power and efficiency with beam currentit clearly indicates that the peak output power and efficiency is around 135.5kW and 20.1%. Figs. 4.9(b) depicts the variation of output power and gain with pitch factor, it clearly

indicates that the peak output power and efficiency is around 135.2kW and 41.3dB. Figs. 4.9(c) depicts the variation of output power with frequencies, indicates that it well matched. The 3dB bandwidth has been found around 6%.

4.5. PIC Simulation of a W-band Fundamental Harmonic Gyro-TWT Amplifier

4.5.1. *PIC Interaction Waveguide Modelling*

In the gyro-devices, the most common interaction region is a cylindrical shape because of symmetry because coupling between beam-wave is high. Progressively, these cylindrical waveguides are being loaded with either by a continuous application of absorber [Chu *et al.* (1999)], or by ceramic loads applied periodically to induce a smooth resistive loss [Calame *et al.* (2002)], or a periodically to act as severs. In the present work, the interaction circuit of the W-band gyro-TWT is being loaded with distributed loss to suppress the potential gyro-backward oscillation. This loaded interaction circuit has been modelled as shown in Fig.4.10.

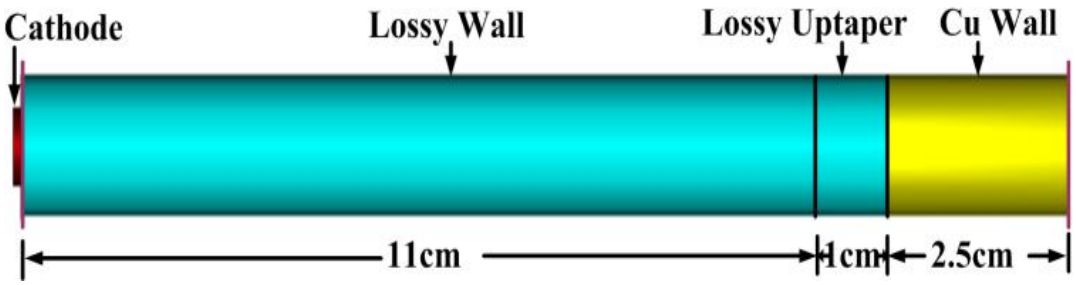

Figure 4.10. Sectional view of the simulation model of heavy loaded W-band gyro-TWT.

The interaction region consists of two parts namely long lossy and the conducting unloaded sections. First, 12cm of the 14.5cm long circular has been loaded with high resistive loss. The region of interest has been discretized using hexahedral (legency) meshing technique and which is very robust even for most complex imported geometries and also which increases the speed of computations with good accuracy.

4.6. Result and Discussion

In order to ensure that the device operation is at the desired mode and frequency, beam absent simulation is performed. Further, for the beam present simulation, the electrons are being considered as uniformly distributed in azimuthal direction in the form of gyrating beamlets and their evolution along the interaction length in the presence of electromagnetic signal is observed in time domain. The space charge effect of the electron beam has been neglected in the PIC simulation for ease of work. Electrons start to bunch as they drift along the interaction region. Once the electrons are bunched, they transfer their energy to electric field which reverses its direction in each half cycle of the cyclotron frequency in synchronism with the Larmor gyration of the electrons. This makes possible amplification of an electromagnetic wave at the cyclotron frequency. The Fourier transform of time varying field confirmed the desired frequency of operation in hot beam analysis. The total length of the interaction circuit has been extended by introducing a loaded section, which allows a high gain and stable operation of the gyro-TWT.

4.6.1. *Beam Absent* (*Cold*) *Simulation*

Figs. 4.11 (a) and (b) show the tranverse cross section of electric field pattern inside the dielectric heavy loaded gyro amplifier. Fig. 4.11(c) shows longitudinal electric field distribution of the desired mode along the axial direction. The red color represents the positive direction of the longitudinal electric field. The accelerating and retarding electronic fields distribute periodically along the longitudinal direction. This is just a requisite for the beam–wave interaction of RF wave amplification mechanism. Proper and meticulous selection of the waveguide dimension will provide the lowest attenuation for the desired operating TE_{01} mode while maintaining a strong enough attenuation of the competing

potentially unwanted modes in order to ensure stable gyro-TWT operation.

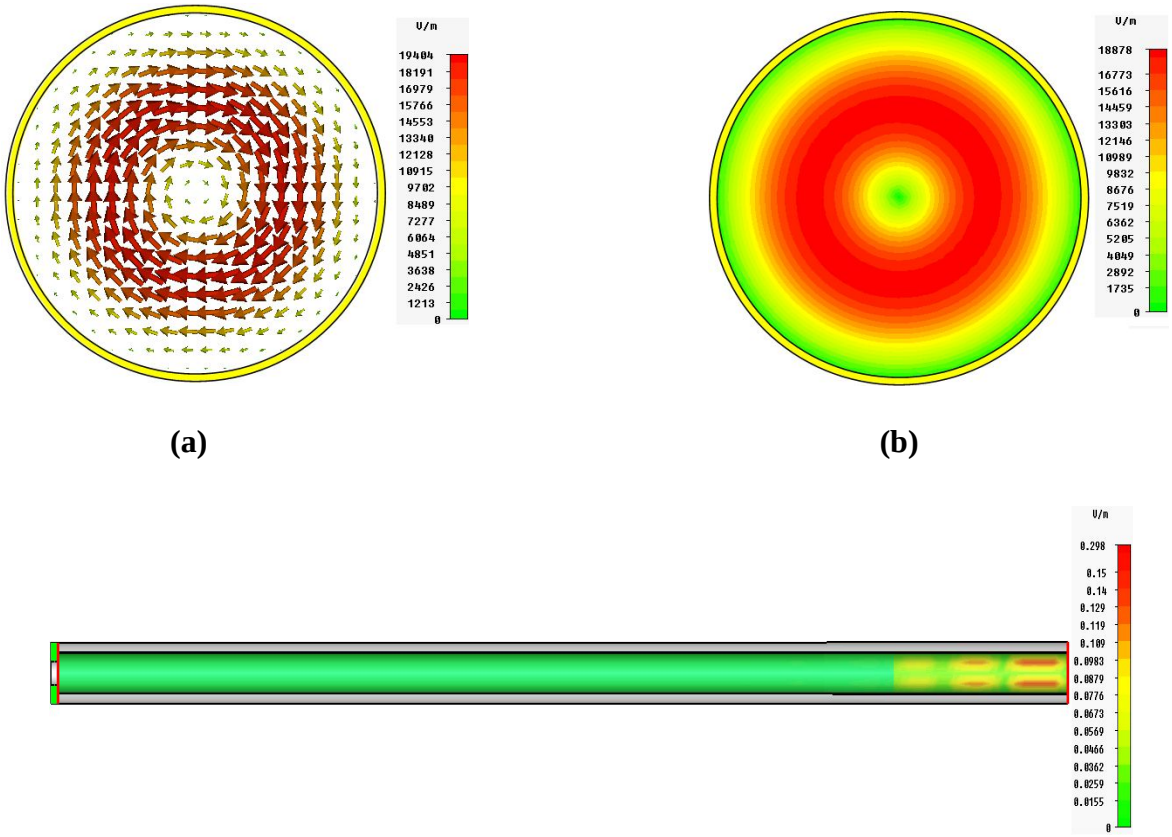

(a) **(b)**

(c)

Figure 4.11. (a) Vector plot of electric field pattern, **(b)** Contour plot of electric field pattern, and **(c)** Side view of the contour of fundamental W-band gyro-TWT amplifier.

4.6.2. *Beam Present* (*Hot*) *Simulation*

The circuit interaction region (both loaded and unloaded section) and output port has been a physical model of the heavily loaded gyro-TWT in order to make it stable. The spiraling electron beam is produced by the current density source. The EM field action changes the electron relativistic factor (γ), depending on the electron phase relative to the wave, and results in phase slippage and bunching, with the corresponding current driving the wave in turn.

4.6.3. *Electron Beam Bunching*

As the EM wave and the gyrating electron beam move down the interaction space, the kinetic energy of the electron beam is transferred to the electromagnetic fields, hence the amplification. The amplified EM is emitted out through the output port where the electron is terminated. Particles have been directly absorbed on the surface of metal neglecting secondary electron emission. The magnetic field is one of the crucial factors in the beam wave interaction. It determines the coupling strength of the beam wave interaction.

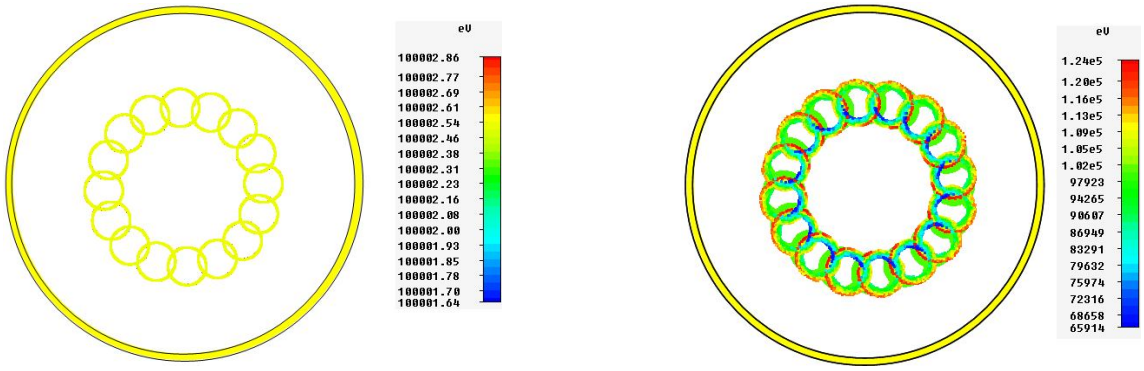

(a) **(b)**

Figure 4.12. Front view of electron beamlets **(a)** initial Interaction, **(b)** after interaction of W-band gyro-TWT.

An increase in magnetic field may enhance the output power at higher frequency but reduce the output power at the lower frequency due to the excessive saturation of the beam wave interaction. Furthermore, an increase in magnetic field will lead to instability of the gyro-TWT amplifier. Additionally, in the present case, a uniform longitudinal magnetic field of 3.56T has been used here to lead the spiraling electron beam. Table 3.1 shows the specification of a gyro-TWT which is used for PIC simulation. The simulation time has been set as 100ns which are good enough for amplifier stability and ninty modes have been taken into account to show the mode competition phenomena in a W-band gyro-TWT.

Subsequently, 3-D CST PIC code has been used to substantiate the beam-wave simulation behavior.

In order to improve the accuracy of the PIC simulation, one should choose the mess size optimally. The lines per wavelength and the mess size should be kept small so as to have good accuracy along with less simulation time. We have used automatic mess generation technique in which lines per wavelength has been set. The automated mess generation provides minimum mess step size 0.0351 mm and maximum step size 0.318987mm which correspond to 3,153,856 number of mess cells. The interaction process electron bunches are formed by interacting with the transverse electric field and also which shows the phase variation of the electrons form the input port to the output port during the interaction process. Fig. 4.12(a) shows that at the entrance of the interaction circuit the electronic transverse momentum has been uniformly distributed which means that macro particles have the same energy and uniform phase distribution and also shows that the Larmor radius of all beamlets is same. After beam-wave interaction, a center of bunch has been formed and the electrons are not uniformly distributed on the gyrating orbit and this is depicted in Fig. 4.14(b). This is enhanced in the loaded section of the interaction region and in the nonlinear amplification region the driver wave is getting amplified while the electrons lose their kinetic energy. The driver signal to the input is around 2W. After the beam-wave interaction, electric field at 92GHz is monitored and TE_{01} mode of operation is observed. The desired mode stable output is obtained at output port and the output power of competing mode is very low.

4.6.4. *Output RF Signal and Power*

The evolution of the EM signal at the output port of the interaction circuit with

respect to time has been shown in Figs. 4.13 for the desired mode TE_{01} (shown as orange colour) and other nearby competing modes TE_{11}, TE_{21} and TE_{02} shown as green, blue and black colour respectively. Moreover, the Figs. 4.14 shows the stable power distribution around 135.2kW at the desired TE_{01} mode. It is important to note that the backward modes TE_{11}, TE_{21} and TE_{02} is dangerous for the stability of gyro-TWT and which has been grown below 100Watts. It is an benifit of the distributed lossy interaction structure. After the template based post processing the output power has been calculated around 135.2kW which has been shown in Fig.4.14.

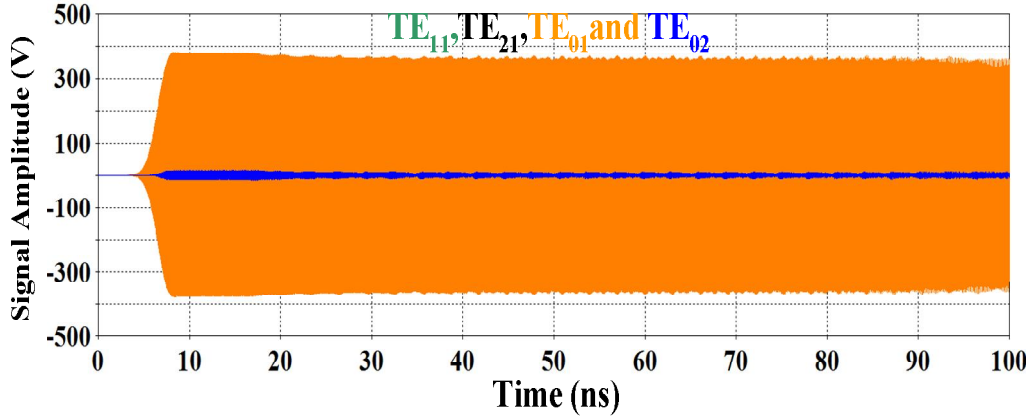

Figure 4.13. Temporal response of signal amplitude for operating and various nearby competing modes.

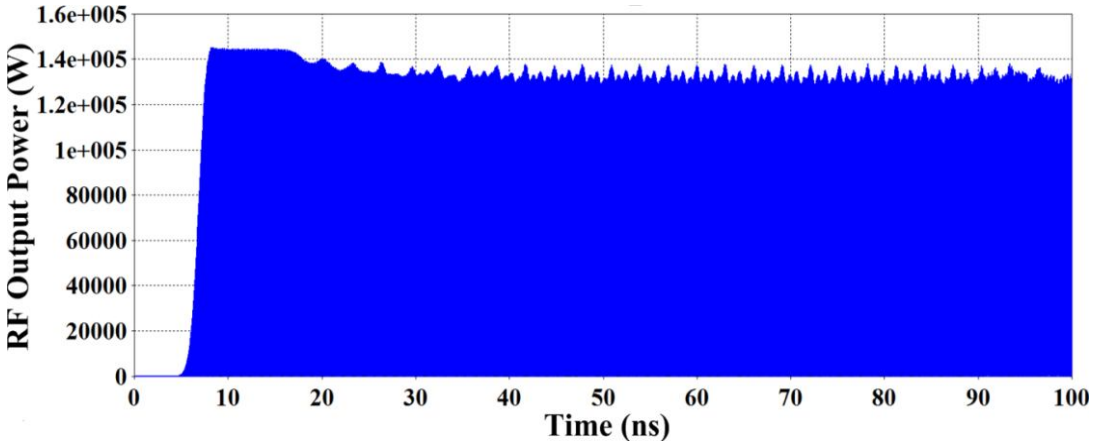

Figure 4.14. Temporal output power growth of W-band gyro-TWT amplifier.

Figs. 4.15(a) displays the axial conour plot and figs. 4.15(b) shows wave particle transfer curve. The Figs. 4.15(c) shows the probe electic field at both input and output ports which are maximum at the desired frequency of operation. In Figs. 4.15 (d), the frequency spectrum of azimuthal electric field has been shown which is obtained by taking the Fourier transform of the electric field. Obviously, it is characterized by a single-frequency component, peaked at 92GHz. This validates the frequency of operation of the proposed gyro-TWT.

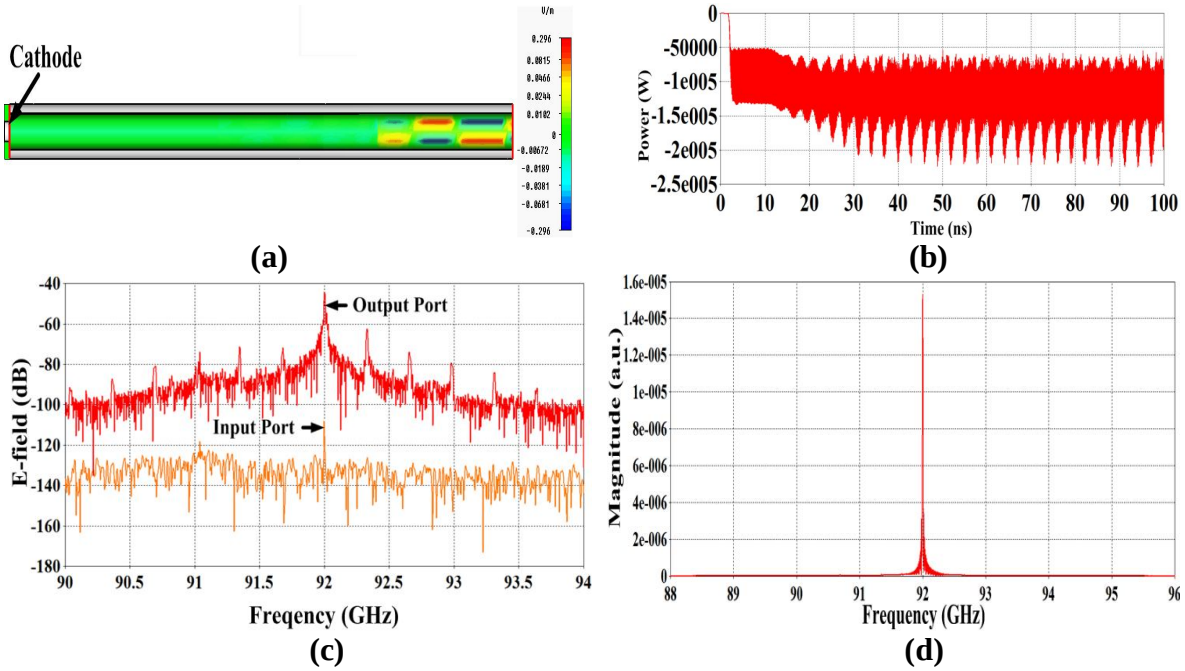

Figure 4.15. (a) Contour plot electric field pattern of TE_{01} mode along the propagation direction **(b)** Wave particle power transfer for W-band gyro-TWT, **(c)** Electric field developed at input and output ports, and **(d)** Fourier Transform spectrum depicts the operating point of a fundamental harmonic gyro-TWT at 92GHz.

4.6.5. *Parametric Analysis and Validation*

The sensitivity of RF output power of the device on the parameters like input power, pitch factor and input frequencies has been studied with the help CST PIC simulation. The variation of the output power with respect to the input power for different velocity spreads

is shown in Figs. 4.16(a). The RF output power is gradually decreasing with respect to increments in the velocity spread. The saturated RF output power is around 172.4kW,

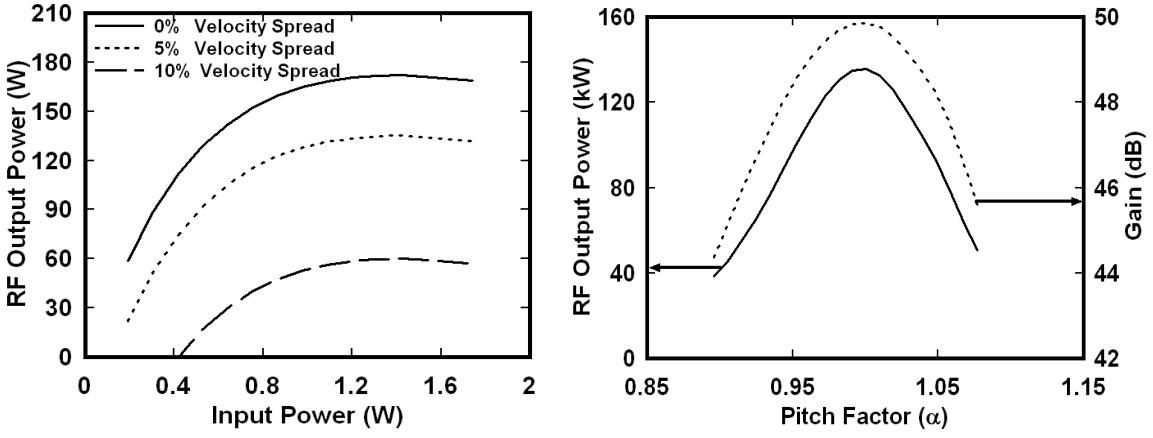

Figure 4.16. (a) Variation of RF output power with drive RF power for different velocity spread, and **(b)** Variation of RF output power and gain with pitch factor.

135.2kW and 59.3kW at 0%, 5%, and 10% velocity spread. The effect of pitch factor on the RF output power and gain of the device is shown in Figs. 4.26(b). For the desired pitch factor, the RF output power and gain levels are optimum. The RF output power and gain is around135.2kW and 49.8dB respectively.

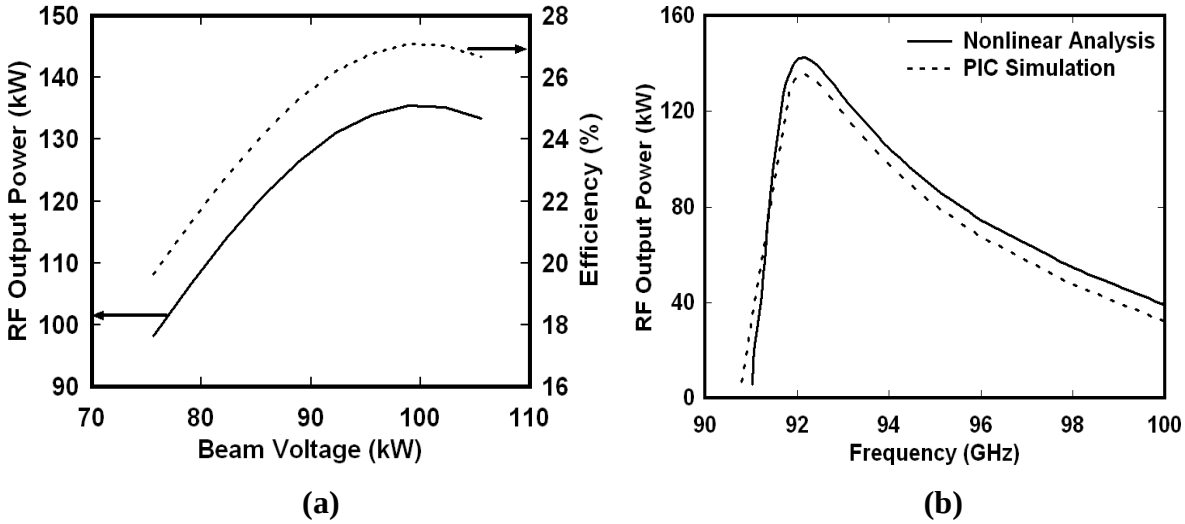

Figure 4.17. (a) Variation of RF output power and efficiency with beam voltage, and (b) Variation of RF output power with driver frequencies.

Figure 4.17 shows the variation of RF output power and gain with beam voltage. It clearly indicates that the peak value is around 135.2kW and gain around 27%. In order validate the analysis described in chapter 3, i.e. figure 4.17(b) depicts the comparison of results obtained through PIC simulation and analysis with respect to frequency. Both are in good agreement to each other and 3dB bandwidth has been found around 5%.

4.7. Conclusion

In this chapter, the beam-wave interaction mechanism of the gyro-TWT has been studied through PIC simulation. Typically, two previously reported gyro-TWT of Ka and W-band, operating at the fundamental harmonic TE_{01} mode has been chosen for this purpose. A commercial available 3D PIC code "CST Particle Studio" has been reconfigured for the typical gyro-TWT structural and beam parameter. The effects of the beam parameters, such as, input current, pitch factor and driver frequency on the performance have been studied, for a typical conventional Ka-band gyro-TWT operating in the TE_{01} circular mode and driven by 71 kV, 9.5A beam. The simulation results shows that the efficiency, gain and the 3dB bandwidth ~ 20.1, 41.3dB and 6%, respectively, for the 0% axial velocity spread in the beam.

In the simulation of heavily loaded W-Band fundamental harmonic TE_{01} mode structure is resistive loaded with taper. The simulation predicted a saturated RF output power of ~135.2kW in TE_{01} mode at 92GHz with an electronic efficiency around 27.04%, for 100kV, 5A annular electron beam having the pitch of 1.0 and the axial beam spread of 5%. The saturated gain has been obtained as about 49.8dB with an instantaneous bandwidth of ~ 5%. Additionally, the 3D PIC results are validated through the self-consistent

nonlinear analytical values and found in agreement within 5%. Further, the CST 3D PIC simulation proves a new effective method to the research of backward wave oscillations.

In the next chapter, the design aspects and stability study of the gyro-TWT amplifier has been carried out. For this purpose a W-band second harmonic gyro-TWT amplifier is typically selected and device design and its stability study will be made. The anlytical results obtained will also be validated though PIC simulation.